HHS Public Access

Author manuscript

J Immunol. Author manuscript; available in PMC 2017 October 15.

Published in final edited form as:

J Immunol. 2016 October 15; 197(8): 3360–3370. doi:10.4049/jimmunol.1502522.

Signaling and Immunoresolving Actions of Resolvin D1 in Inflamed Human Visceral Adipose Tissue

Esther Titos[*,§], **Bibiana Rius**[*], **Cristina López-Vicario**[*], **José Alcaraz-Quiles**[*], **Verónica García-Alonso**[*], **Aritz Lopategi**[*], **Jesmond Dalli**[‖], **Juan José Lozano**[§], **Vicente Arroyo**[†], **Salvadora Delgado**[‡], **Charles N. Serhan**[‖], and **Joan Clària**[*,§,¶]

[*]Department of Biochemistry and Molecular Genetics, University of Barcelona, Barcelona, 08036, Spain

[‡]Department of Gastrointestinal Surgery, Hospital Clínic-IDIBAPS, University of Barcelona, Barcelona, 08036, Spain

[§]Centro de Investigación Biomédica en Red de Enfermedades Hepáticas y Digestivas (CIBERehd), University of Barcelona, Barcelona, 08036, Spain

[†]European Foundation for the Study of Chronic Liver Failure (EF-CLIF), University of Barcelona, Barcelona, 08036, Spain

[¶]Department of Biomedical Sciences, University of Barcelona, Barcelona, 08036, Spain

[‖]Center for Experimental Therapeutics and Reperfusion Injury, Department of Anesthesiology, Perioperative and Pain Medicine, Brigham and Women's Hospital and Harvard Medical School, Boston, MA 02115, USA

Abstract

Persistent activation of the innate immune system greatly influences the risk of developing metabolic complications associated with obesity. In this study, we explored the therapeutic potential of the specialized pro-resolving mediator (SPM) resolvin D1 (RvD1) to actively promote the resolution of inflammation in human visceral adipose tissue from obese patients. By means of LC-MS/MS-based metabololipidomic analysis we identified unbalanced production of SPMs (i.e. D- and E-series resolvins, protectin D1, maresin 1 and lipoxins) with respect to inflammatory lipid mediators (i.e. leukotriene B_4 and prostaglandins) in omental adipose tissue from obese patients. In parallel, high-throughput transcriptomic analysis revealed a unique signature in this tissue characterized by an overactivation of the interleukin (IL)-10 signaling pathway. Incubation of inflamed obese visceral adipose tissues and human macrophages with RvD1 limited the excessive activation of the IL-10 pathway by reducing phosphorylation of signal transducer and activator of

Corresponding Authors: Esther Titos (Tel: 34-93-2275400 ext 4536; esther.titos@ciberehd.org). Joan Clària (Tel: 34-93-2275400 ext 1798; jclaria@clinic.ub.es).

Contact Address: Dr. Esther Titos, Department of Biochemistry and Molecular Genetics, CIBERehd-Hospital Clínic, Villarroel 170, Barcelona 08036, Spain, Tel: 34-93-2275400 ext 4536, esther.titos@ciberehd.org and/or Dr. Joan Clària, Department of Biochemistry and Molecular Genetics, Hospital Clínic, Villarroel 170, Barcelona 08036, Spain, Tel: 34-93-2275400 ext 1798, jclaria@clinic.ub.es

DISCLOSURES

C.N.S. is an inventor on several patents [resolvins] assigned to BWH and licensed to Resolvyx Pharmaceuticals; scientific founder of Resolvyx Pharmaceuticals with equity ownership in the company; and has interests reviewed and managed by the BWH and Partners HealthCare in accordance with their conflict of interest policies.

transcription (STAT) proteins. Of interest, RvD1 blocked STAT-1 and its target inflammatory genes (i.e. CXCL9) as well as persistent STAT3 activation without affecting the IL-10 anti-inflammatory response characterized by inhibition of IL-6, IL-1β, IL-8 and TNFα. Furthermore, RvD1 promoted resolution by enhancing the expression of the IL-10-target gene heme oxygenase-1 by mechanisms depending on p38 mitogen-activated protein kinase (MAPK) activity. Together, our data show that RvD1 can tailor the quantitative and qualitative responses of human inflamed adipose tissue to IL-10 and provide a mechanistic basis for the immunoresolving actions of RvD1 in this tissue. These findings may have potential therapeutic implications in obesity-related insulin resistance and other metabolic complications.

INTRODUCTION

A chronic state of low-grade inflammation in adipose tissue is recognized as a critical factor for the progression of metabolic complications associated with obesity, such as insulin resistance and non-alcoholic fatty liver disease (NAFLD) (1,2). Indeed, these obesity-related comorbidities are closely linked to the presence of a persistent activation of pro-inflammatory signaling pathways in adipose tissue, which severely disrupts key metabolic checkpoints in this tissue (1,2). Among these signals, enhanced production of pro-inflammatory adipokines such as tumor necrosis factor (TNF) α, interleukin (IL)-6, IL-1β, monocyte chemoattractant protein-1 (MCP-1), leptin and resistin, accompanied by a reduction in the anti-inflammatory adipokine, adiponectin, are common findings in obese individuals with the metabolic syndrome (3,4).

In addition to the heightened production of inflammatory mediators, obese adipose tissue shows an intrinsic inability to resolve uncontrolled inflammation and to restore tissue homeostasis and functionality (5). Current evidence indicates that inflammation does not switch off in a passive manner but involves a program of unique endogenous mechanisms and mediators that orchestrate its active resolution in a timely and effective manner (6). Among these, lipid mediators such as lipoxins, resolvins, protectins and maresins, collectively known as specialized-proresolving mediators (SPM) have attracted the most attention (7). SPM act not only as ‘braking signals’ of the persistent vicious cycle leading to unremitting inflammation, but mainly as promoters of active resolution of inflammation. Indeed, at the preclinical level, therapeutic administration of SPM has been shown to promote resolution of inflamed adipose tissue and to protect mice against obesity-associated complications such as insulin resistance and NAFLD (8–12). An interesting aspect of these mediators is that SPM are able to take advantage of macrophage plasticity by inducing changes in the phenotype of recruited adipose tissue macrophages toward a pro-resolution M2 state (8,10). In addition, SPM enhance the emergence of pro-resolving macrophages expressing low levels of CD11b and producing the anti-inflammatory cytokine IL-10 (13). Moreover, SPM induce monocyte differentiation into phagocytosing macrophages, facilitating the removal of dead or dying cells (efferocytosis) and enhancing phagocyte efflux to drain lymph nodes in order to aid in clearing out the inflamed tissues (14,15). All these processes are considered to positively contribute to the resolution of adipose tissue inflammation and the prevention of metabolic syndrome in obesity.

The present study was undertaken to move forward in the concept of resolution as an active phenomenon aimed at suppressing uncontrolled inflammation in human obese adipose tissue. This study has three main objectives: 1) to translate the findings obtained in pre-clinical models to real-world human samples of adipose tissue from obese individuals; 2) to characterize the intracellular signaling pathways by which SPM may exert pro-resolving actions in inflamed adipose tissue in a series of mechanistic studies in human adipose tissue and macrophages; and 3) to provide proof of concept that targeting SPM signaling pathways is worthy of further investigation. Through experiments with the representative SPM resolvin D1 (RvD1), here we provide evidence that SPM promote pro-resolutive responses in inflamed human adipose tissue by interacting with the signaling pathways of IL-10 and by modulating the archetypal anti-inflammatory response of this cytokine.

MATERIALS AND METHODS

Study participants and sample collection

Forty-one individuals with obesity undergoing laparoscopic bariatric surgery and seven patients without a history of obesity undergoing laparoscopic cholecystectomy were recruited from the Gastroenterology Surgery Unit of the Hospital Clínic of Barcelona and included in the study. Participants were selected according to their BMI calculated as mass/height^2 and categorized as non-obese controls (BMI < 29.9 kg/m^2, n=7) and obese (BMI > 29.9 kg/m^2, n=41). Individuals with inflammatory bowel disease or cancer and obese patients with previous bariatric surgery were excluded from the study. Harvested omental adipose tissue samples were washed twice with DPBS and minced in ≈100 mg pieces, placed in either 10% formalin or snap-frozen in liquid nitrogen and stored at −80°C for further analysis. Demographic, clinical data and drug use were collected from patients' electronic medical records. All studies were conducted in accordance with the criteria of the Investigation and Ethics Committee of the Hospital Clínic and written informed consent was obtained from all participants (protocol #2012-7239).

Biochemical analyses

Serum concentrations of glucose, cholesterol, TAG, ALT and AST were determined by standard laboratory procedures.

Immunohistochemistry analysis

The tissues were routinely fixed in 10% buffered formalin, embedded in paraffin and sectioned into 2 μm-thick sections for CD68 immunohistochemistry with the Dako Flex Ready-to-use monoclonal mouse anti-human CD68 antibody (Dako) and H&E counterstain at the Pathology Department of the Hospital Clínic. For quantitative analysis, the number of CD68-positive cells was counted in a total of 15 high-power fields (HPFs) per tissue section under a light microscope (Nikon Eclipse E600 microscope) at x400 magnification, and results were given as number of positive cells/HPF.

Adipose tissue explants and "ex vivo" incubations

human visceral adipose tissue from obese patients was collected under sterile conditions and placed in a P100 plate with pre-warmed (37°C) DPBS containing antibiotics (penicillin (100

U/ml) and streptomycin (100 μg/ml)). Connective tissue and blood vessels were removed by dissection before cutting the tissue into small pieces (60–80 mg). Explants were washed with DPBS at 37°C by centrifugation for 1 min at 400*g* to remove blood cells and then maintained overnight in culture in DMEM with L-glutamine (2 mM), antibiotics and 10% FBS. Treatments were performed after a gentle rinse in DPBS containing penicillin and streptomycin, in DMEM with L-glutamine, antibiotics and 1% endotoxin-free BSA-fatty acid free (FAF) (Sigma). Protein and mRNA expression were assessed in explants incubated with vehicle (0.01% EtOH) or RvD1 (1, 10 and 50 nM) (Cayman Chemicals) for 30 min followed by the addition of cytokines (IL-10, 20 ng/ml; IL-1β, 25 pg/ml and IL-6, 10 ng/ml) (R&D Systems) for 0.5, 2 and 6 h at 37°C. For experiments assessing IL-10 production, adipose tissue was preincubated with 5 μM SB203580 (p38 MAPK inhibitor XVI) (Merck Millipore) in the presence of RvD1 (1, 10 and 50 nM) for 30 min before the addition of LPS (1 μg/ml) (Sigma) for 24 h. At the end of the incubation periods, supernatants were collected and explants were frozen in liquid nitrogen, placed into polypropylene tubes and stored at −80°C for further analysis.

Isolation of adipocytes and stromal vascular cells (SVC)

Adipose tissue samples (3–7 g) were extensively washed with sterile DPBS containing antibiotics to remove contaminating blood cells. The specimens were then cut carefully in 0.6–1.0 g pieces avoiding connective tissue and blood vessels. Explants were washed with DPBS at 37°C by centrifugation for 1 min at 400*g* to remove blood cells. Tissue was finely minced and placed in 5 ml of digestion buffer containing Krebs Ringer supplemented with 1.5% BSA-FAF and 2.5 mg/ml of Liberase (Roche Diagnostics) and incubated at 37°C for 45 min with gentle shaking. Tissue homogenates were filtered through a 100 μm nylon mesh and maintained in Krebs Ringer supplemented with 1.5% BSA-FAF and 2 mM EDTA for 10 min. Floating cells (adipocytes) were collected, homogenized in 1 ml of TRizol Reagent (Invitrogen) and stored at −80°C for futher analysis. The infranatant containing the SVC was centrifuged at 500*g* for 5 min and pelleted cells were homogenized in 1 ml of TRizol Reagent and kept at −80°C until futher analysis.

Cell culture and cell incubations

The human monocyte cell line, THP-1 (ATCC, Manassas, VA) was cultured with RPMI 1640 medium containing 10% FBS and antibiotics at 37°C in a 5% CO_2 incubator. Before performing the experiments, the growth medium was exchanged for serum-free RPMI 1640 medium for 18h. In some experiments, unstimulated THP-1 cells or THP-1 cells differentiated into macrophage-like cells by the addition of PMA (50 ng/ml) (Sigma) for 48 h were seeded (8×10^5–1×10^6) into 12- and 24-well plates, and then incubated at 37°C in serum-free RPMI 1640 medium in the presence of vehicle (0.01% EtOH) and RvD1 (1, 10 and 50 nM) for 30 min followed by the addition of increasing concentrations of IL-10 (2, 20, 100 and 200 ng/ml), IL-6 (0.05, 10 and 20 ng/mL) and IL-1β (25 pg/ml) for 10 min. An additional time point of 6 h was performed for IL-10 treatments. For experiments assessing SOCS3 stabilization, THP-1 cells were pre-incubated with or without IL-10 (20 ng/ml) for 30 min before the addition of IL-6 (10 ng/ml) in the presence or absence of 10 μM of the proteasome inhibitor MG132 (Calbiochem, Merck Millipore) for 5 h. To verify the effects of MG132 in preventing the proteolytic degradation of newly synthesized SOCS3 by the

ubiquitin–proteasome system (16) aditional experiments were performed in THP-1 cells pre-incubated in the absence or presence of MG132 (10 μM) for 30 min before the addition of IL-6 (10 ng/ml) for 5 h. In some experiments, LPS stimulation was performed in the presence of a mouse monoclonal anti-human IL-10 receptor (10 μg/ml) or control non-immune mouse immunoglobin (IgG) (R&D Systems). At the end of the incubation periods, cells and supernatants were collected for futher analysis.

RNA isolation, reverse transcription and real-time PCR

Isolation of total RNA from adipose tissue, adipocytes, SVC and THP-1 cells was performed using the TRIzol reagent. RNA concentration was assessed in a NanoDrop-1000 spectrophotometer (NanoDrop Technologies), and its integrity tested with a RNA 6000 Nano Assay in a Bioanalyzer 2100 (Agilent Technologies). cDNA synthesis from 0.5–1 μg of total RNA was performed using the High-Capacity cDNA Archive Kit (Applied Biosystems). Real-time PCR analysis of SOCS1 (Hs00705164_s), SOCS3 (Hs02330328_s1), IL-1β (Hs01555410_m1), IL-8 (Hs00174103_m1), IL-6 (Hs00985639_m1), IL-6 signal transducer (ST) (Hs00174360_m1), IL-6 receptor (R) alpha (Hs01075666_m1), cyclooxygenase (COX)-2 (Hs00153133_m1), TNFα (Hs01113624_g1), IL-10 (Hs00961622_m1), CD163 (Hs00174705_m1), heme oxygenase (HO)-1 (Hs01110250_m1), HO-2 (Hs01558390_m1), CXCL9 (Hs00171065_m1) and CXCL10 (Hs01124251_g1) was performed in a 7900HT Fast System (Applied Biosystems) using β-actin (Hs99999903_m1) as the endogenous control. PCR results were analyzed with Sequence Detector 2.1 software (Applied Biosystems). Relative quantification of gene expression was performed using the comparative Ct method. The amount of target gene, normalized to β-actin and relative to a calibrator, was determined by the arithmetic equation $2^{-\Delta\Delta Ct}$, as described in the comparative Ct method (http://docs.appliedbiosystems.com/pebiodocs/04303859.pdf). For the analysis of real-time PCR data from patients, a total RNA derived from normal human adipose tissue pooled from 18 individuals (Clontech Laboratories, Inc) was used as a calibrator.

Western blot analysis

Total protein was extracted using a lysis buffer containing 50 mM HEPES, 20 mM β-glycerophosphate, 2 mM EDTA, 1% Igepal, 10% glycerol, 1 mM $MgCl_2$, 1 mM $CaCl_2$, and 150 mM NaCl for adipose tissue and a modified RIPA buffer containing 50 mM Tris-HCl, 150 mM NaCl, 1% Igepal, and 0.25% 1 mM EDTA for THP-1 cells, both supplemented with protease and phosphatase inhibitors from Roche Diagnostics (Complete Mini and PhosSTOP cocktails, respectively). Homogenates were incubated on ice for 10 min and centrifuged at either 14000*g*, 15 min (cells) or 16000*g*, 40 min (tissue) at 4 °C. Total protein (30–40 μg) from supernatants was placed in SDS-containing Laemmli sample buffer, heated for 5 min at 95°C, and separated by 12% SDS-PAGE for 120 min at 120 V. Transfer was performed by the iBlot Dry Blotting System (Invitrogen) onto PVDF membranes at 20 V over 7 min, and the efficiency of the transfer was visualized by Ponceau S staining. The membranes were then soaked for 1 h at room temperature in 0.1% T-TBS and 5% (w/v) nonfat dry milk. Blots were washed 3 times for 5 min each with 0.1% T-TBS and subsequently incubated overnight at 4°C with primary anti-human antibodies for HO-1, SOCS3, phospho-STAT1 (Tyr701), phospho-STAT3 (Tyr705), phospho-p38 MAPK

(Thr180/Tyr 182), STAT1, STAT3 and p38 MAPK, all purchased from Cell Signaling. Thereafter, the blots were washed 3 times for 5 min each with 0.1% T-TBS containing 5% (w/v) nonfat dry milk and incubated for 1 h at room temperature with donkey anti-rabbit (Biolegend) or anti-mouse (Cell Signaling) HRP-linked antibody (1:2000) in 0.1% T-TBS. Bands were visualized using the EZ-ECL chemiluminescence detection kit (Biological Industries). To assess housekeeping protein expression, membranes were reblotted overnight at 4°C with primary rabbit anti-human GAPDH antibody (Imgenex) or β-actin HRP conjugate (Cell Signaling) and detected and visualized as described above. Total STAT1, STAT3, p38 MAPK, GAPDH or β-actin were used as an internal control to verify basal level expression and equal protein loading.

High-throughput transcriptomic analysis

RNA profiling was conducted in adipose tissue samples from 4 patients with morbid obesity and 4 control subjects using the Affymetrix Human Genome U219 expression array plate containing more than 36,000 transcripts and variants (Affymetrix, Inc.). Preparation of cRNA probes, hybridization, and scanning of arrays were performed according to the manufacturer's protocol and carried out by the Functional Genomics Unit of IDIBAPS. Affymetrix gene expression data were normalized with the robust multiarray algorithm using a custom probe set definition that maps probes directly to Entrez Gene Ids (HGU219_Hs_ENTREZG). A filtering step excluding probes not reaching a coefficient of variation of 0.02 was employed and the total number of obtained probes was 13,928. For the detection of differentially expressed genes, a linear model was fitted to the data and empirical Bayes moderated statistics were calculated using the Limma package (Bioconductor). Adjustment of p-values was done by the determination of false discovery rates (FDR) using the Benjamini-Hochberg procedure (17). All computations were done using R statistical software. Genes representing a fold change of 1.5 or greater and a moderated p-value <0.05 were considered as differentially expressed. Microarray data has been deposited in Gene Expression Omnibus (GEO): GSE7141 (http://www.ncbi.nlm.nih.gov/genbank).

Metabololipidomics using liquid chromatography-tandem mass spectrometry (LC-MS/MS)

Adipose tissues were suspended in 1.0 mL cold methanol, gently homogenized then kept on ice for 1 h to allow for protein precipitation. Lipid mediators were profiled as described in (18). Briefly, lipid mediators were extracted by solid phase extraction using C18 columns and eluted using methyl formate. Fractions were then taken for LC-MS/MS-based lipidomics using a QTrap 6500 (ABSciex) MS-MS coupled to a Shimadzu HPLC system. Calibration curves were obtained using synthetic and authentic lipid mediators mixtures. Linear calibration curves for each were obtained with r^2 values in the range 0.98–0.99. Quantification was carried out based on the peak area of the MRM transition and the linear calibration curve for each compound or compounds with similar physical properties.

Luminex xMAP technology

Cytokine levels were determined in cell culture supernatants (25 μl) using a multiplexed bead-based immunoassay Milliplex MAP Human Cytokine/Chemokine Magnetic Bead Panel (Merck Millipore) on a Luminex 100 Bioanalyzer. The readouts were analyzed with

the standard version of the Milliplex Analyst software (Merck Millipore). A five-parameter logistic regression model was used to create standards curves (pg/mL) and to calculate the concentration of each sample.

Measurement of IL-10 levels

Levels of IL-10 in supernatants from adipose tissue explants were determined by a specific enzyme-linked immunoassay (Human IL-10 ELISA kit, Invitrogen).

Statistical analysis of the results was performed using the unpaired Student t test. For multivariate statistical analysis, partial least squares-discriminant analysis (PLS-DA) was performed using SIMCA 13.0.3 software (Umetrics) following mean centering and unit variance scaling of lipid mediator amounts. Results were expressed as means ± SEM, and differences were considered significant at a p value ≤ 0.05.

RESULTS

The demographic and clinical characteristics of the patients included in the study are shown in Supplementary Table 1. Obese individuals had increased body weight, body mass index (BMI) and serum triglyceride (TAG) levels and a higher incidence of hepatic steatosis (Supplementary Table 1). There were no statistically significant differences in gender, serum glucose, cholesterol, alanine aminotransferase (ALT) and aspartate aminotransferase (AST) levels between the two study cohorts. The obese cohort was younger than the non-obese group (Supplementary Table 1). As typical of obesity, this cohort presented a greater incidence of type II diabetes and hypertension and took antihypertensive (beta-blockers, ACE inhibitors and angiotensin II receptor antagonists) and antidiabetic (metformin and glimepiride) drugs at higher frequency than the non-obese control (CT) group.

We first performed gene expression profiling by microarray analysis of omental adipose tissue from obese (Ob) (BMI>29.9) and non-obese CT (BMI<29.9) individuals. High-throughput transcriptome and subsequent functional analyses identified a group of genes associated with the inflammatory process that was differentially modulated in obesity (Figure 1A). Among these, we found a significative up-regulated fold change in the expression of genes involved in IL-10 signaling, including IL-10 (1.77, $P<0.0005$), its receptor (IL-10RA) (1.5, $P<0.05$) and downstream targets such as HO-1 (2.23, $P<0.05$) and CD163 (1.84, $P<0.05$) (Figure 1A). These changes were associated with a high inflammatory burden (i.e. over-expression of IL-6 and IL-1β) in obese adipose tissue (Figure 1A). Over-expression of cytokines/adipokines was confirmed by real-time PCR (Figure 1B). COX-2 was also significantly up-regulated in adipose tissue from obese subjects (Supplementary Figure 1A). Finally, as compared to the CT group, omental adipose tissue from Ob patients showed an increased macrophage content, as revealed by CD68 immunostaining (Figure 1C). Increased macrophage infiltration was confirmed by real-time PCR analysis of this macrophage marker, the expression of which increased gradually in a BMI-dependent manner (Figure 1D).

We next profiled the levels of bioactive lipid mediators in visceral adipose tissue samples by LC-MS/MS-based metabolo-lipidomics. Human visceral adipose tissue produced the full

spectra of SPM derived from endogenous sources of DHA (i.e. D-series resolvins, protectin D1 and maresin 1), EPA (i.e. E-series resolvins) and arachidonic acid (lipoxin (LX) A_4 and AT-LXA_4). These mediators were identified in according to published criteria that include matching retention times (Figure 2A) and at least six characteristic and diagnostic ions for each as illustrated with results obtained for RvD1 (Figure 2B). Visceral adipose tissue also had detectable levels of arachidonic-acid derived 5-lipoxygenase (5-LO) products (i.e. leukotriene (LT) B_4 and its all-trans isomer 5(S),12(S)-dihydroxy-6,10-trans-8,14-cis-eicosatetraenoic acid (5,12-diHETE), prostaglandins (PGs) (i.e. PGE_2, PGD_2, and $PGF_{2\alpha}$) and thromboxane (TX) A_2 (Figure 2A). Quantitation of lipid mediators in obese and non-obese adipose tissue is given in Supplementary Table 2. Notably, adipose tissue samples from obese patients showed a reduced ratio of SPM production with respect to both 5-LO products (i.e. LTB_4 and its all-trans isomer) and PGs (Figure 2C). To further interrogate the lipid mediator profiles obtained from obese and non-obese adipose tissue we employed data driven modeling. Partial least square discriminant analysis (PLS-DA) of these lipid mediator profiles demonstrated that profiles obtained from obese patients gave a distinct cluster in principle component 1 (Figure 2D, **left panel**). The loading plot demonstrated that pro-resolving mediators including RvD1 and RvD5 as well as the inflammation initiating eicosanoids LTB_4 and TXB_2 associate with profiles obtained from obese adipose tissues with variable importance in projection scores > 1 whereas RvD2 and RvD3 were associated with profiles from control patients (Figure 2D, **right panel**). Interestingly, multiple linear regression analysis identified a close relationship between SPM and IL-10 and between IL-10 and CD68 in adipose tissue (Figure 2E). SPM levels did not correlate with IL-1β and IL-6 (Supplementary Figure 1B). On the other hand, tissue levels of LTB_4 and its all-trans isomer correlated with IL-10 and IL-1β expression (Supplementary Figure 1C), whereas levels of PGs only correlated with IL-10 (Supplementary Figure 1D).

To understand how cytokines/adipokines influence adipose tissue inflammation and how this can be modulated by SPM, we next performed *ex vivo* experiments in adipose tissue explants from obese patients. As shown in Figure 3A, addition of recombinant human IL-10 to fat explants exerted anti-inflammatory properties by decreasing the expression of IL-6, IL-1β, IL-8 and TNFα. Addition of IL-1β produced an opposite effect and induced the expression of inflammatory cytokines/adipokines (Figure 3B). In contrast, obese adipose tissue was not responsive to IL-6 stimulation (Figure 3C). On the other hand, IL-10 enhanced its own expression in adipose tissue in a statistically significant manner (Figure 3D), whereas this autoregulatory loop was not seen with IL-1β and IL-6 (data not shown). The IL-10 positive feedback loop was also present in human THP-1 macrophages (Figure 3E). These cells were selected on the basis that they provide an optimal platform to perform mechanistic studies in one of the predominant immune cell types present in the SVC fraction of the adipose tissue. Indeed, as compared to adipocytes, cells of the SVC fraction were the major contributors to cytokine/adipokine production in visceral fat from obese individuals (Figure 3F). Another characteristic observed in obese fat explants was that IL-10 was able to induce the expression of CD163 and HO-1, which are part of the IL-10-induced anti-inflammatory response (19) (Figure 3G). HO-2 was also up-regulated by IL-10 (Supplementary Figure 2A). Moreover, the HO-1 mRNA response to IL-10 was amplified in adipose tissue explants from obese patients incubated with RvD1 at 10 nM (Figure 3H).

Similarly, RvD1 at 1 nM amplified in an additive fashion the IL-10-induced HO-1 protein expression after 120 min of incubation (Figure 3I). Unexpectedly, RvD1 at high concentrations (> 10 nM) reduced HO-1 protein expression in adipose tissue explants (Figure 3I). RvD1 did not modify CD163 expression either in resting or IL-10 treated adipose tissue explants (Supplementary Figure 2B). The strengthening of the IL-10-mediated HO-1 response induced by RvD1 was confirmed in human THP-1 macrophages (Figure 3J).

To identify signaling events that may mediate RvD1 actions on the IL-10-induced anti-inflammatory response, we next investigated the canonical IL-10/signal transducer and activator of transcription 3 (STAT3) pathway in obese adipose tissue. As shown in Figure 4A, human adipose tissue showed a constitutive phosphorylation on the Tyr705 residue of STAT3, being the extent of activation significantly higher in obese individuals than in non-obese CT subjects. Consistent with the fact that IL-10 response is preserved in obese adipose tissue, this cytokine activated $STAT3^{Tyr}$ phosphorylation after 120 min of stimulation (Figure 4B). Notably, pretreatment with RvD1 at 1 nM significantly sensitized adipose tissue to IL-10 and shifted the maximal induction of $STAT3^{Tyr}$ phosphorylation to the left and upward at 30 min (Figure 4C). In contrast, RvD1 significantly reduced IL-10-induced $STAT3^{Tyr}$ phosphorylation at higher concentrations (10 and 50 nM) and for longer periods of time (120 min) (Figure 4C). Importantly, the IL-10-induced anti-inflammatory response (characterized by inhibition of IL-6, IL-1β, IL-8 and TNFα) was preserved in adipose tissue during RvD1 treatment, and this SPM even further reduced IL-8 expression (Supplementary Figure 2C). A concentration-dependent increase in $STAT3^{Tyr}$ phosphorylation in response to IL-10 and its down-regulation by RvD1 were confirmed in human THP-1 macrophages (Figure 4, D and E).

In addition to IL-10, other cytokines such as IL-6 use receptor-induced signaling through the JAK/STAT3 pathway. Paradoxically, and in contrast to IL-10, IL-6 produces an opposed transcriptional and pro-inflammatory response (20). For this reason, we next explored whether RvD1 was able to modulate $STAT3^{Tyr}$ phosphorylation of obese fat explants exposed to IL-6. Consistent with the lack of response of obese adipose tissue to IL-6, this cytokine/adipokine was totally ineffective in inducing the phosphorylation of $STAT3^{Tyr}$ in this human tissue, a response that was not modified by RvD1 (Figure 5A). Since in contrast to IL-10, STAT3 activation by IL-6 is negatively regulated by the suppressor of cytokine signaling 3 (SOCS3), a member of the family of SH2-containing E3 ligases (21), this lack of effectiveness could be related to the observed SOCS3 up-regulation in obese adipose tissue (Figure 5B). Similar up-regulation was detected in the high-throughput transcriptome analysis (5.3 fold in obese versus control non-obese, $P<0.05$). Moreover, a close direct relationship was identified between SOCS3 and IL-6 by multiple linear regression in human adipose tissue (Supplementary Figure 2D). Given that SOCS3 as well as SOCS1 are predominantly expressed in the SVC fraction of visceral adipose tissue from obese individuals (Figure 5C), we performed mechanistic studies in human THP-1 cells. In these cells and in contrast to that seen in obese adipose tissue, IL-6 produced the expected induction in $STAT3^{Tyr}$ phosphorylation (Figure 5D). As a proof of concept that SOCS3 is involved in the blunted response to IL-6, we obtained data showing that this canonical response of IL-6 signaling disappears in the presence of MG132, a proteasome inhibitor that

has the ability to stabilize SOCS3 in response to IL-6 (Figure 5, E and F). Nevertheless, the unresponsiveness of obese adipose tissue to IL-6 could be multifactorial depending on different mechanisms because, for instance, the expression of the IL-6 receptor and its transactivator gp130 are significantly down-regulated in visceral adipose tissue of obese individuals (Figure 5G). Recent studies have suggested that in addition to IL-10 and IL-6, the STAT3 pathway is also part of the non-canonical IL-1β signaling pathway (22,23). As shown in Figure 5, H and I, IL-1β was also able to induce $STAT3^{Tyr}$ phosphorylation after 30 min of incubation in visceral obese adipose tissue but not in THP-1 cells. These responses were not significantly modified by RvD1 (Figure 5, H and I).

An excessive over-activation of the IL-10 signaling pathway during type I interferon-derived responses can lead to the undesired activation of the STAT1 and its target inflammatory genes (i.e. CXCL9) (24). As shown in Figure 6A, a remarkable phosphorylation of $STAT1^{Tyr}$ and induction of CXCL9 was observed after incubating obese adipose tissue with IL-10. Importantly, this IL-10-induced $STAT1^{Tyr}$ phosphorylation signal was repressed by RvD1 (Figure 6B). Over-stimulation of the $STAT1^{Tyr}$ pathway by IL-10 was also observed in THP-1 cells incubated with high concentrations (>100 ng/ml) of this cytokine (Figure 6C). Consistently, the expression of STAT1-dependent genes (i.e. CXCL9 and CXCL10) was up-regulated by high IL-10 concentrations (Figure 6D). Similar to that observed in obese adipose tissue, RvD1 attenuated in a concentration-dependent manner IL-10-induced $STAT1^{Tyr}$ phosphorylation in these cells (Figure 6E).

The STAT3 signaling pathway is necessary but not sufficient for the IL-10 anti-inflammatory response, and for instance, this cytokine can induce HO-1 expression in LPS-elicited macrophages via a p38 MAPK pathway (25,26). In view of this, we next investigated the impact of RvD1 on the anti-inflammatory production of IL-10 in response to LPS. As shown in Figure 7A, LPS remarkably up-regulated IL-10, HO-1, IL-6 and IL-8 expression. Of note, LPS-mediated HO-1 induction was blocked by the selective p38 MAPK inhibitor SB203580, confirming that the p38 MAPK signaling pathway is involved in the production of HO-1 (Figure 7A). Under these inflammatory conditions, RvD1 induced a further up-regulation of HO-1, an effect that was also dependent on p38 MAPK signaling (Figure 7B). Consistent with this finding, RvD1 increased the phosphorylation of p38 MAPK in a concentration-dependent manner, an effect that was also blocked by the selective p38 MAPK inhibitor SB203580 (Figure 7C). In parallel with this, RvD1 enhanced IL-10 production (Figure 7D), suggesting that this SPM modulates HO-1 in an IL-10-dependent manner. Consistently, induction of HO-1 by RvD1 was partially blocked by a selective antibody directed against the IL-10 receptor (Figure 7E). Interestingly, measurement of cytokine levels in cell supernatants from these experiments in a multiplex assay revealed that RvD1 is also able to increase in a concentration-dependent manner the secretion of IL-1β receptor antagonist (IL-1ra), a natural inhibitor of the pro-inflammatory actions of IL-1β (27) (Supplementary Figure 2E). The induction of IL-1ra release by RvD1 was also dependent of p38 MAPK activity (Supplementary Figure 2E).

DISCUSSION

The results of the current study move forward the concept that SPM promote resolution and actively suppress uncontrolled inflammation in adipose tissue from obese individuals. In particular, the pro-resolving actions of RvD1 in this tissue are mediated through its interaction with the pathways signaling for IL-10 and through the modulation of the archetypal anti-inflammatory response of this cytokine. The current findings add to previous work in pre-clinical models of obesity showing that RvD1 and other SPM attenuate adipose tissue inflammation by reducing the production of cytokines/adipokines (i.e. TNFα, IL-6 and MCP-1) and shifting the phenotype of recruited macrophages toward the M2 pro-resolving state (8,10–12). Accordingly, the major novelty of the present study is the translation of these therapeutic benefits to the clinical scenario in samples of adipose tissue from obese individuals.

Visceral adipose tissue from obese patients showed an exaggerated expression of both inflammatory and anti-inflammatory cytokines/adipokines. In the same direction, visceral adipose tissue from obese patients showed increased levels of both inflammatory (LTs and PGs) and anti-inflammatory/pro-resolving (SPM) lipid mediators. However, the ratio between SPM production with respect to LTs and PGs was significantly reduced in adipose tissue samples from obese individuals. This observation indicates the presence of a remarkable deficit in SPM levels as compared to pro-inflammatory signals and the existence of an impaired capacity of visceral adipose tissue to resolve uncontrolled inflammation in this condition. These findings are in agreement with those previously reported in other fat depots such as subcutaneous and perivascular fat from patients afflicted by the metabolic syndrome (28). Since visceral adipose is recognized to be central to metabolic diseases and to have a more negative impact on health than other fat depots (29), our data supports the concept that persistent un-resolved inflammation in adipose tissue is one of the most important factors driving the metabolic complications associated with obesity, including insulin resistance and NAFLD (1,2).

Visceral adipose tissue from obese individuals appears to display a characteristic response to the actions of cytokines/adipokines. For example, obese adipose tissue remains sensitive to the inflammatory actions of IL-1β. Similarly, the anti-inflammatory response elicited by IL-10, characterized by inhibition of inflammatory cytokines/adipokines such as IL-6, IL-1β, IL-8 and TNFα, is also preserved in this tissue. In sharp contrast, obese adipose tissue is unresponsiveness to IL-6. Moreover, in the obese adipose tissue, the signal transduction pathways activated by these cytokines/adipokines display a disorganized pattern. For example, STATs are the classical transcription factors transducing the signals elicited by type I and type II cytokine receptors (30). In the case of IL-10, binding of this cytokine to its receptor activates janus kinase (JAK) which is associated with the cytoplasmatic domain of the receptor. The activated receptor-JAK complex then recruits and promotes the tyrosine (Tyr) 705 phosphorylation of STAT3 (pSTAT3^{Tyr}), leading to their homodimerization and subsequent translocation to the nucleus where they bind to STAT3-binding elements of IL-10 responsive-genes (31). The results of the current study support the concept that STAT3 is required, but not sufficient for mediating IL-10-induced anti-inflammatory responses in inflamed obese adipose tissue. In this regard, our findings

identify that the p38 MAPK signaling pathway is involved in the regulation of HO-1 expression. This is in agreement with previous studies proposing p38 MAPK as the pathway signaling the anti-inflammatory responses to IL-10 in murine macrophages (32). Moreover, our findings identify the p38 MAPK signaling pathway as a genuine mechanism underlying the additive anti-inflammatory actions of RvD1 and IL-10 in obese adipose tissue. This observation is in agreement with that reported by Cooray et al (33), establishing that phosphorylation of p38 MAPK is engaged in the pro-resolving signature of ALX activation, the receptor mediating the actions of other SPMs such as LXA_4 and annexin A1. Another example of the peculiarities of obese adipose tissue in terms of activation of signal transduction pathways by cytokines/adipokines is that incubation of fat explants with recombinant IL-1β resulted in the phosphorylation of STAT3, an effect that was not modulated by RvD1. Although other laboratories have demonstrated the activation of STAT3 in response to IL-1β (22,23), unlike IL-10 and IL-6, this is a non-canonical pathway for IL-1β signaling. Finally, the observation that IL-10 at high concentrations induce STAT1 phosphorylation in obese adipose tissue deserves some comment. This is not surprising because an excessive over-activation of the IL-10 signaling pathway during type I interferon-derived responses can lead to the undesired activation of the STAT1 and its target inflammatory genes (i.e. CXCL9 and CXCL10) (24). Of paramount importance is the fact that this IL-10-induced STAT1 phosphorylation is significantly repressed by RvD1, which indicates that in addition to promoting IL-10 anti-inflammatory response, RvD1 plays a role as a braking signal that limits excessive over-activation of the IL-10 signaling pathways. A schematic diagram summarizing most of the actions elicited by IL-10 in obese adipose tissue and the modulation by RvD1 is given in Figure 8.

In summary, our study describes novel signal regulatory mechanisms for RvD1, which culminate in promoting a more intense IL-10-induced anti-inflammatory response in inflamed human adipose tissue. These findings are in accordance with previous studies in other organs, tissues and cells in which RvD1 counter-regulates inflammatory signals while promoting the secretion of anti-inflammatory cytokines (34), thus highlighting the pro-resolving functions of these lipid mediators.

Supplementary Material

Refer to Web version on PubMed Central for supplementary material.

Acknowledgments

We are extremely grateful to both the surgical and nursing staff from the Department of Gastrointestinal Surgery and the Ambulatory Surgery Unit, Hospital Clínic for their professionalism and dedication in providing human samples. The authors also thank Dr. Romain Colas, Brigham and Women's Hospital (BWH)-Harvard Medical School, for expert help with validation of SPM physical properties and LS-MS/MS profiling.

Supported by Spanish MEC (SAF12/32789, SAF15-63674-R and PIE14/00045) under European Regional Development Funds (ERDF) (J.C.) and in part by National Institutes of Health (NIH) grant no. P01GM095467 (C.N.S.). CIBERehd is funded by the Instituto de Salud Carlos III. This study was carried out at the Center Esther Koplowitz. C.L.-V. was supported by IDIBAPS/Fundació Clínic. V.G.-A. and B.R. have fellowships from MEC, A.L. was funded by a Marie Curie Action and J.A.-Q. is a recipient of an Agaur/BFU fellowship (FI-DGR 2015).

Abbreviations used in this paper

ALT	alanine aminotransferase
AST	aspartate aminotransferase
BMI	body mass index
HO	heme oxygenase
HPF	high power field
IL	interleukin
LC-MS/MS	liquid chromatography-tandem mass spectrometry
MAPK	mitogen-activated protein kinase
MRM	multiple reaction monitoring
NAFLD	non-alcoholic fatty liver disease
RvD1	resolvin D1
STAT	signal transducer and activator of transcription
SPM	specialized pro-resolving mediators
SVC	stromal vascular cells
SOCS	suppressor of cytokine signaling
TAG	triglyceride

References

1. Ferrante AW Jr. Obesity-induced inflammation: a metabolic dialogue in the language of inflammation. J Intern Med. 2007; 262:408–414. [PubMed: 17875176]
2. Hotamisligil GS. Inflammation and metabolic disorders. Nature. 2006; 444:860–867. [PubMed: 17167474]
3. Ouchi N, Parker JL, Lugus JJ, Walsh K. Adipokines in inflammation and metabolic disease. Nat Rev Immunol. 2011; 11:85–97. [PubMed: 21252989]
4. Chawla A, Nguyen KD, Goh YP. Macrophage-mediated inflammation in metabolic disease. Nat Rev Immunol. 2011; 11:738–749. [PubMed: 21984069]
5. Spite M, Clària J, Serhan CN. Resolvins, specialized proresolving lipid mediators, and their potential roles in metabolic diseases. Cell Metab. 2014; 19:21–36. [PubMed: 24239568]
6. Gilroy DW, Lawrence T, Perretti M, Rossi AG. Inflammatory resolution: new opportunities for drug discovery. Nat Rev Drug Discov. 2004; 3:401–416. [PubMed: 15136788]
7. Serhan CN. Pro-resolving lipid mediators are leads for resolution physiology. Nature. 2014; 510:92–101. [PubMed: 24899309]
8. Hellmann J, Tang Y, Kosuri M, Bhatnagar A, Spite M. Resolvin D1 decreases adipose tissue macrophage accumulation and improves insulin sensitivity in obese-diabetic mice. FASEB J. 2011; 25:2399–2407. [PubMed: 21478260]
9. González-Periz A, Horrillo R, Ferré N, Gronert K, Dong B, Morán-Salvador E, Titos E, Martínez-Clemente M, López-Parra M, Arroyo V, Clària J. Obesity-induced insulin resistance and hepatic

steatosis are alleviated by omega-3 fatty acids: a role for resolvins and protectins. FASEB J. 2009; 23:1946–1957. [PubMed: 19211925]

10. Titos E, Rius B, González-Périz A, López-Vicario C, Morán-Salvador E, Martínez-Clemente M, Arroyo V, Clària J. Resolvin D1 and its precursor docosahexaenoic acid promote resolution of adipose tissue inflammation by eliciting macrophage polarization toward an M2-like phenotype. J Immunol. 2011; 187:5408–5418. [PubMed: 22013115]
11. Clària J, Dalli J, Yacoubian S, Gao F, Serhan CN. Resolvin D1 and resolvin D2 govern local inflammatory tone in obese fat. J Immunol. 2012; 189:2597–2605. [PubMed: 22844113]
12. Rius B, Titos E, Morán-Salvador E, López-Vicario C, García-Alonso V, González-Périz A, Arroyo V, Clària J. Resolvin D1 primes the resolution process initiated by calorie restriction in obesity-induced steatohepatitis. FASEB J. 2014; 28:836–848. [PubMed: 24249635]
13. Schif-Zuck S, Gross N, Assi S, Rostoker R, Serhan CN, Ariel A. Saturated-efferocytosis generates pro-resolving CD11b low macrophages: modulation by resolvins and glucocorticoids. Eur J Immunol. 2011; 41:366–379. [PubMed: 21268007]
14. Serhan CN, Savill J. Resolution of inflammation: the beginning programs the end. Nat Immunol. 2005; 6:1191–1197. [PubMed: 16369558]
15. Schwab JM, Chiang N, Arita M, Serhan CN. Resolvin E1 and protectin D1 activate inflammation-resolution programmes. Nature. 2007; 447:869–874. [PubMed: 17568749]
16. Wiejak J, Dunlop J, Mackay SP, Yarwood SJ. Flavanoids induce expression of the suppressor of cytokine signalling 3 (SOCS3) gene and suppress IL-6-activated signal transducer and activator of transcription 3 (STAT3) activation in vascular endothelial cells. Biochem J. 2013; 454:283–293. [PubMed: 23782265]
17. Ritchie ME, Phipson B, Wu D, Hu Y, Law CW, Shi W, Smyth GK. limma powers differential expression analyses for RNA-sequencing and microarray studies. Nucleic Acids Res. 2015; 43:e47. [PubMed: 25605792]
18. Colas RA, Shinohara M, Dalli J, Chiang N, Serhan CN. Identification and signature profiles for pro-resolving and inflammatory lipid mediators in human tissue. Am J Physiol Cell Physiol. 2014; 307:C39–C54. [PubMed: 24696140]
19. Abraham NG, Drummond G. CD163-Mediated hemoglobin-heme uptake activates macrophage HO-1, providing an antiinflammatory function. Circ Res. 2006; 99:911–914. [PubMed: 17068296]
20. El Kasmi KC, Holst J, Coffre M, Mielke L, de PA, Lhocine N, Smith AM, Rutschman R, Kaushal D, Shen Y, Suda T, Donnelly RP, Myers MG Jr, Alexander W, Vignali DA, Watowich SS, Ernst M, Hilton DJ, Murray PJ. General nature of the STAT3-activated anti-inflammatory response. J Immunol. 2006; 177:7880–7888. [PubMed: 17114459]
21. Yoshimura A, Naka T, Kubo M. SOCS proteins, cytokine signalling and immune regulation. Nat Rev Immunol. 2007; 7:454–465. [PubMed: 17525754]
22. Radtke S, Wuller S, Yang XP, Lippok BE, Mutze B, Mais C, de Leur HS, Bode JG, Gaestel M, Heinrich PC, Behrmann I, Schaper F, Hermanns HM. Cross-regulation of cytokine signalling: pro-inflammatory cytokines restrict IL-6 signalling through receptor internalisation and degradation. J Cell Sci. 2010; 123:947–959. [PubMed: 20200229]
23. Mori T, Miyamoto T, Yoshida H, Asakawa M, Kawasumi M, Kobayashi T, Morioka H, Chiba K, Toyama Y, Yoshimura A. IL-1beta and TNFalpha-initiated IL-6-STAT3 pathway is critical in mediating inflammatory cytokines and RANKL expression in inflammatory arthritis. Int Immunol. 2011; 23:701–712. [PubMed: 21937456]
24. Pike KA, Hutchins AP, Vinette V, Theberge JF, Sabbagh L, Tremblay ML, Miranda-Saavedra D. Protein tyrosine phosphatase 1B is a regulator of the interleukin-10-induced transcriptional program in macrophages. Sci Signal. 2014; 7:ra43. [PubMed: 24803538]
25. O'Farrell AM, Liu Y, Moore KW, Mui AL. IL-10 inhibits macrophage activation and proliferation by distinct signaling mechanisms: evidence for Stat3-dependent and -independent pathways. EMBO J. 1998; 17:1006–1018. [PubMed: 9463379]
26. Lee TS, Chau LY. Heme oxygenase-1 mediates the anti-inflammatory effect of interleukin-10 in mice. Nat Med. 2002; 8:240–246. [PubMed: 11875494]
27. Arend WP, Malyak M, Guthridge CJ, Gabay C. Interleukin-1 receptor antagonist: role in biology. Annu Rev Immunol. 1998; 16:27–55. [PubMed: 9597123]

28. Clària J, Nguyen BT, Madenci AL, Ozaki CK, Serhan CN. Diversity of lipid mediators in human adipose tissue depots. Am J Physiol Cell Physiol. 2013; 304:C1141–C1149. [PubMed: 23364264]
29. Wajchenberg BL, Giannella-Neto D, da Silva ME, Santos RF. Depot-specific hormonal characteristics of subcutaneous and visceral adipose tissue and their relation to the metabolic syndrome. Horm Metab Res. 2002; 34:616–621. [PubMed: 12660870]
30. Schindler C, Levy DE, Decker T. JAK-STAT signaling: from interferons to cytokines. J Biol Chem. 2007; 282:20059–20063. [PubMed: 17502367]
31. Villarino AV, Kanno Y, Ferdinand JR, O'Shea JJ. Mechanisms of Jak/STAT signaling in immunity and disease. J Immunol. 2015; 194:21–27. [PubMed: 25527793]
32. Ashwell JD. The many paths to p38 mitogen-activated protein kinase activation in the immune system. Nat Rev Immunol. 2006; 6:532–540. [PubMed: 16799472]
33. Cooray SN, Gobbetti T, Montero-Melendez T, McArthur S, Thompson D, Clark AJ, Flower RJ, Perretti M. Ligand-specific conformational change of the G-protein-coupled receptor ALX/FPR2 determines proresolving functional responses. Proc Natl Acad Sci U S A. 2013; 110:18232–18237. [PubMed: 24108355]
34. Croasdell A, Thatcher TH, Kottmann RM, Colas RA, Dalli J, Serhan CN, Sime PJ, Phipps RP. Resolvins attenuate inflammation and promote resolution in cigarette smoke-exposed human macrophages. Am J Physiol Lung Cell Mol Physiol. 2015; 309:L888–L901. [PubMed: 26301452]

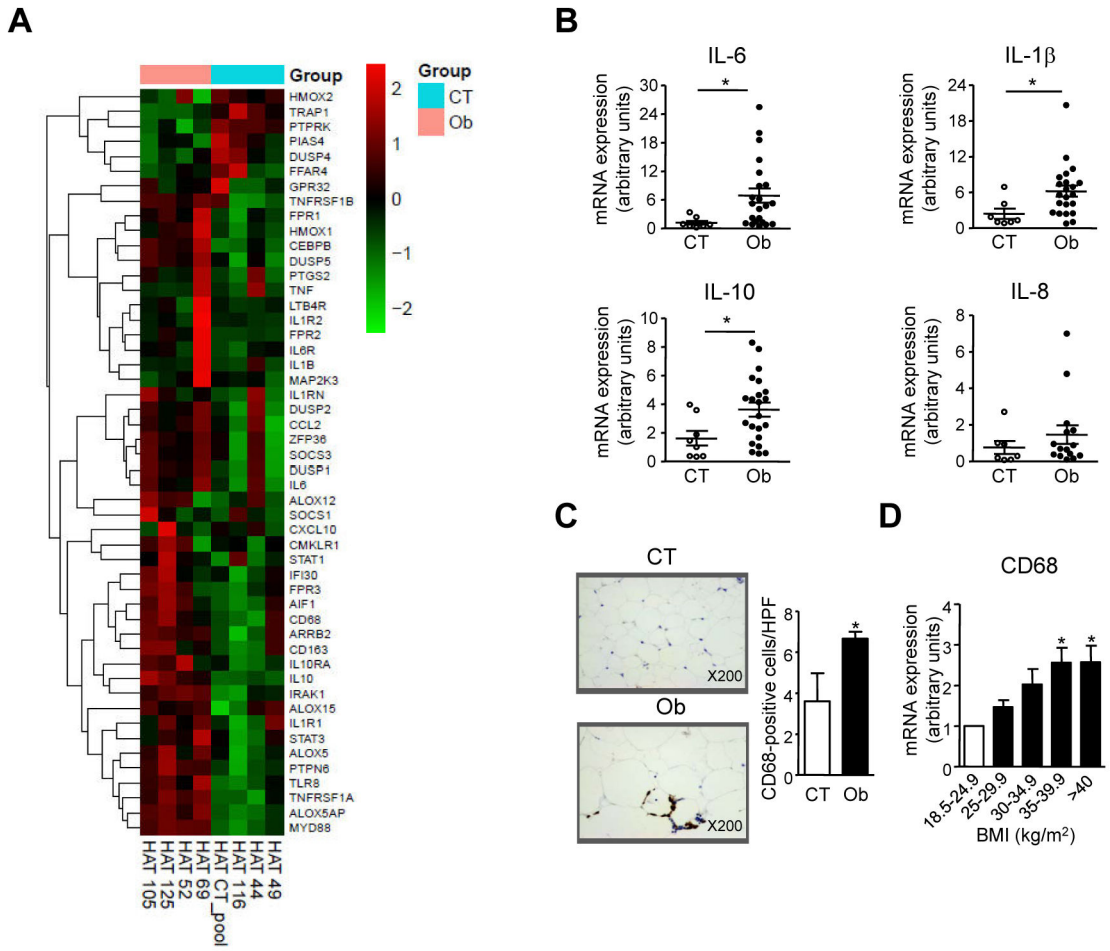

Figure 1. High-throughput transcriptome analysis of human obese visceral adipose tissue

(A). Upregulated expression of inflammation-related genes (Affymetrix Human Genome U219 expression array plate) in visceral adipose tissue from obese (Ob) and non-obese control (CT) subjects. Results are expressed as a matrix view of gene expression data (heat map) where rows represent genes and columns represent hybridized samples. The intensity of each color denotes the standardized ratio between each value and the average expression of each gene across all the samples. Red pixels correspond to an increased abundance of mRNA in the human adipose tissue samples indicated, whereas green pixels indicate decreased mRNA levels. **(B)** Relative mRNA levels for interleukin (IL)-6, IL-1β, IL-10 and IL-8 in human adipose tissue from CT (n=8) and Ob (n=22) subjects were assessed by real-time PCR**. (C)** Representative photomicrographs (original magnification, X200) of adipose tissue sections stained with the macrophage marker CD68 in control (CT, BMI<29.9) and obese (Ob, BMI>29.9) individuals. Number of CD68-positive cells per HPF in human adipose tissue sections from CT (n=3) and Ob (n=10) subjects is shown on the right. **(D)** Adipose tissue CD68 gene expression in relation to BMI (n=20) was analyzed by real-time PCR. Pooled human adipose tissue RNA from 18 healthy subjects served as a calibrator. Results are expressed as mean ± SEM. *, P<0.05 vs CT subjects.

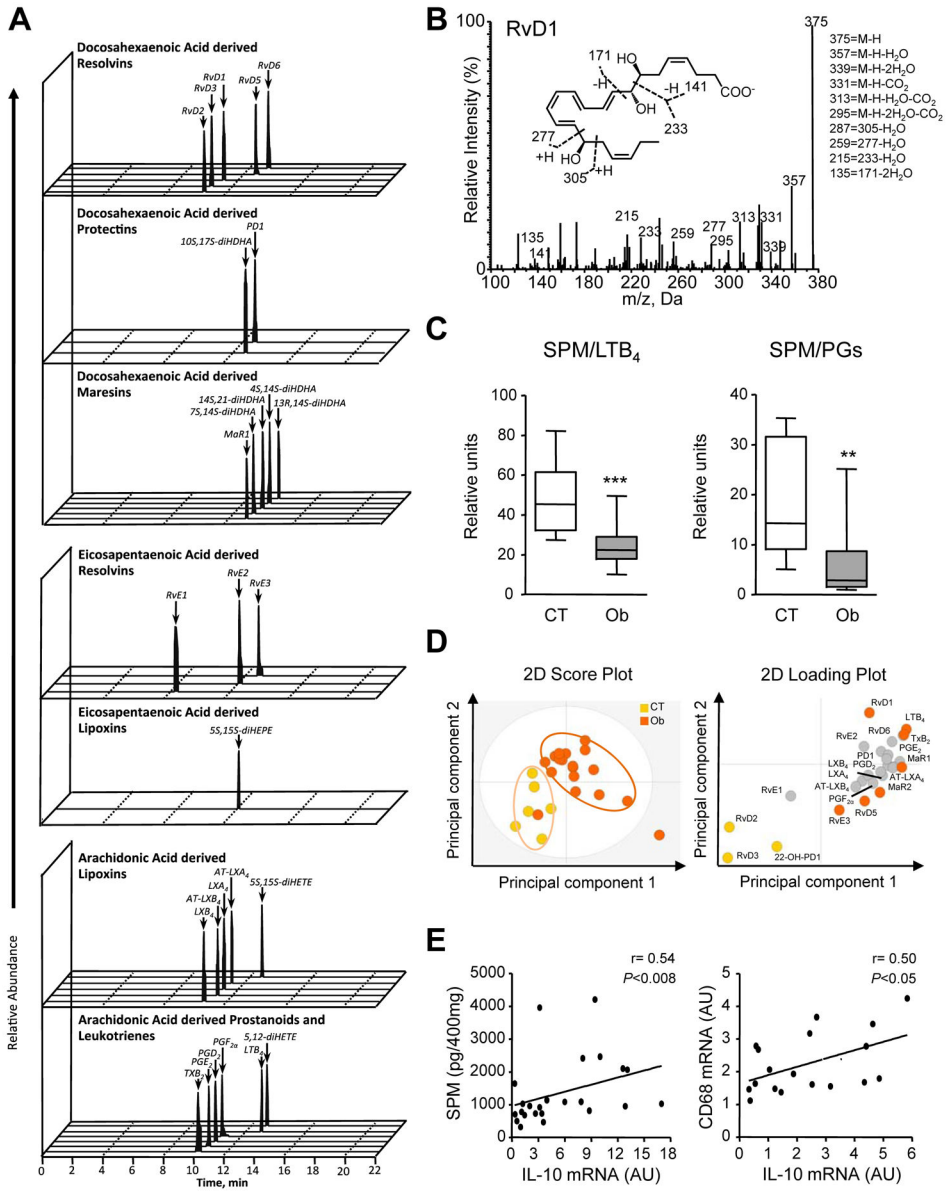

Figure 2. Distinct lipid mediator-SPM signature profiles in visceral adipose tissues from obese and non-obese patients

(A) Representative multiple reaction monitoring (MRM) chromatograms obtained by LC-MS/MS-based metabololipidomics of selected ion pairs for DHA, EPA and AA-derived lipid mediators. Results are representative of n=24 adipose tissue samples. **(B)** Tandem mass spectra employed in the identification of RvD1. **(C)** Ratios of specialized pro-resolving mediators (SPM) to LTB_4 (including its all-trans isomer) and prostaglandins (PGs) in human adipose tissue from CT (n=6) and Ob (n=18) individuals. **(D)** Partial least square discriminant analysis of lipid mediator profiles from obese and non-obese adipose tissue. **(E)** Correlations (Spearman's rho test) between SPM and IL-10 and between CD68 and IL-10 in human visceral adipose tissue. Results are expressed as mean ± SEM. **, P<0.005 and ***, P< 0.001 vs CT subjects.

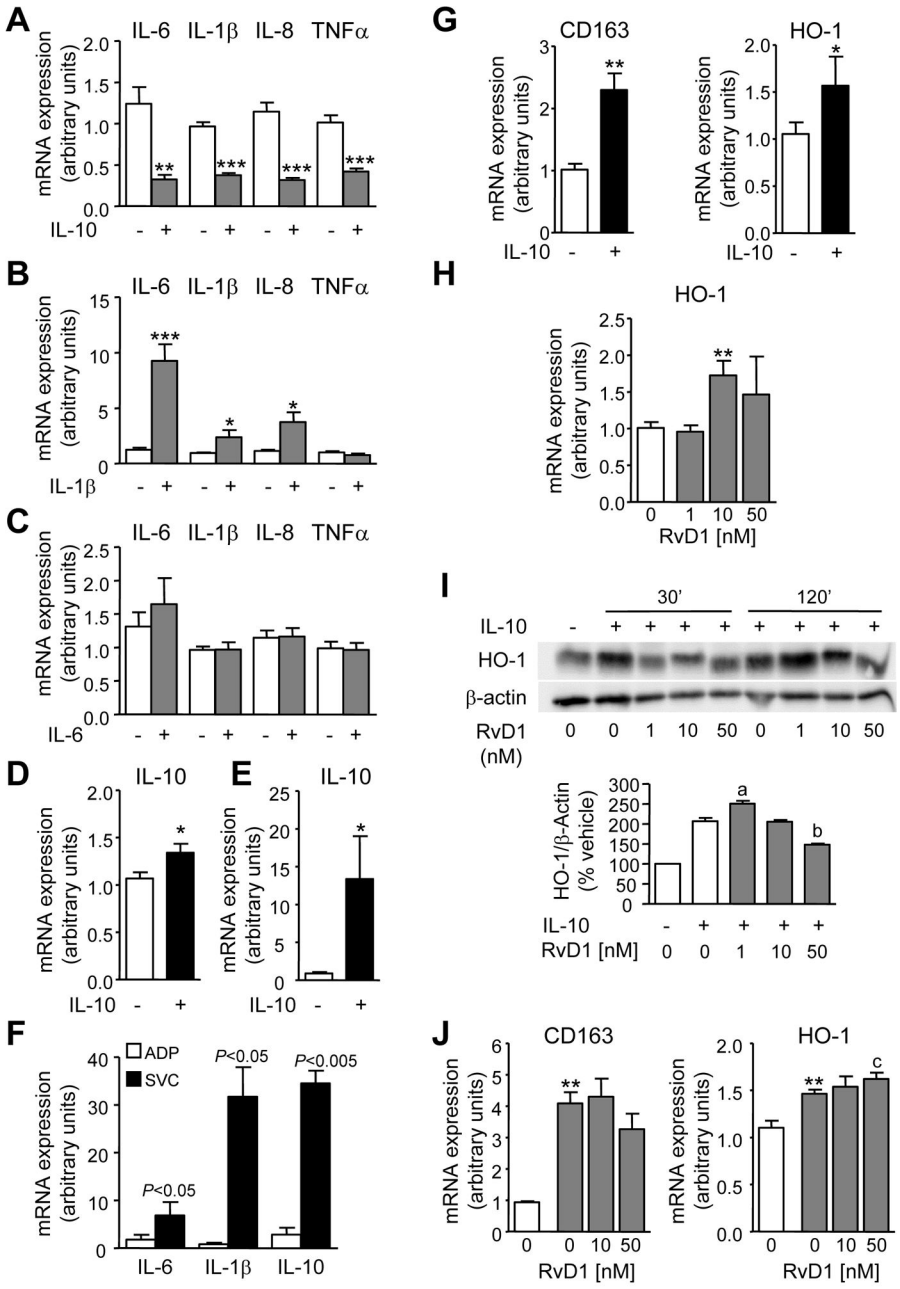

Figure 3. RvD1 potentiates IL-10-induced HO-1 expression in human obese adipose tissue and macrophages

(A) Relative mRNA levels for IL-6, IL-1β, IL-8 and TNFα in obese adipose tissue cultured explants incubated for 6 h in the absence (−) or presence (+) of IL-10 (20 ng/ml). **(B)** Changes in gene expression in response to IL-1β (25 pg/ml). **(C)** Changes in gene expression in response to IL-6 (10 ng/ml). **(D)** Changes in IL-10 mRNA expression in obese adipose tissue explants incubated with IL-10 (20 ng/ml). **(E)** mRNA expression for IL-10 in THP1-derived macrophages incubated with IL-10 (20 ng/ml) for 6 h. **(F)** mRNA expression for IL-6, IL-1β, and IL-10 was analyzed in adipocytes (ADP) and stromal vascular cells (SVC) isolated from human obese adipose tissue. **(G)** Relative mRNA expression for the

anti-inflammatory genes CD163 and HO-1 in obese adipose tissue explants incubated for 6 h in the absence (−) or presence (+) of IL-10 (20 ng/ml). **(H)** Changes in HO-1 mRNA expression in response to increasing concentrations of RvD1 (0, 1, 10 and 50 nM). **(I)** Representative immunoblot of HO-1 protein expression (upper panel) assessed by western blot in obese adipose tissue explants in the presence of increasing concentrations of RvD1 (0, 1, 10 and 50 nM) for 30 min followed by addition of IL-10 (20 ng/ml) for 30 or 120 min. Densitometric analysis at 120 min is shown below. Results are expressed as mean ± SEM of n=3 independent experiments performed in duplicate. *P* values are given vs ADP. *, $P<0.05$, **, $P<0.005$ and ***, $P<0.0005$ vs non-treated adipose tissue explants. a, $P<0.05$ and b, $P<0.005$ for RvD1 vs IL-10-treated explants at time 120 min. c, $P<0.05$ vs IL-10-treated cells.

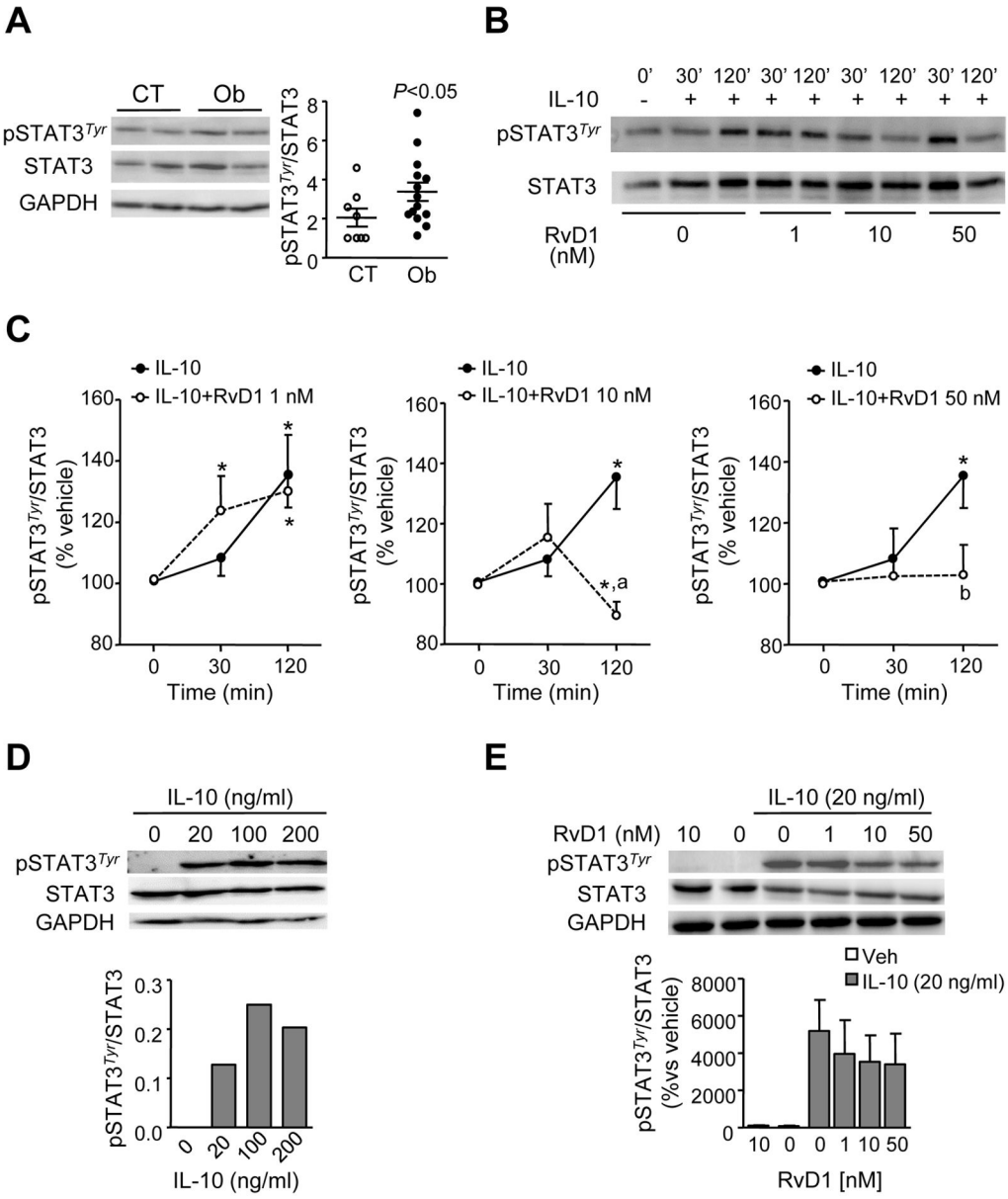

Figure 4. RvD1 modulates IL-10-induced STAT3 activation

(A) Representative immunoblot of STAT3 and phospho-STAT3 (pSTAT3, phosphorylation at Tyr705, pSTAT3^{Tyr}) assessed by western blot in visceral adipose tissue samples from control (CT, n=8) and obese (Ob, n=14) individuals. The densitometric analysis of pSTAT3^{Tyr} to total STAT3 ratio is shown on the right. **(B)** Representative immunoblots of pSTAT3^{Tyr} and total STAT3 levels in adipose tissue explants incubated with increasing concentrations of RvD1 (0, 1, 10 and 50 nM) for 30 min followed by the addition of IL-10 (20 ng/ml) for 30 or 120 min. **(C)** Kinetic analysis of STAT3^{Tyr} phosphorylation in adipose tissue explants incubated in the absence (solid circles) or presence (empty circles) of RvD1 and stimulated with IL-10. **(D)** Representative immunoblots analyzing STAT3 activation in THP1 monocytes incubated in the presence of increasing concentrations of IL-10 for 10 min. Densitometric analysis of phosphorylated protein to total protein ratios is shown below. **(E)**

Representative immunoblots of STAT3 and pSTAT3^{Tyr} in THP-1-derived macrophages incubated in the presence of increasing concentrations of RvD1 for 30 min followed by the addition of IL-10 (20 ng/ml) for 10 min. Densitometric analysis of phosphorylated protein to total protein ratios is shown below. Results are expressed as mean ± SEM of n=3 independent experiments performed in duplicate. *P* values are given vs CT. *, $P<0.05$ vs vehicle (0.01% ethanol) at time 0. a, $P<0.05$ and b, $P<0.01$ for RvD1 vs vehicle at time 120 min.

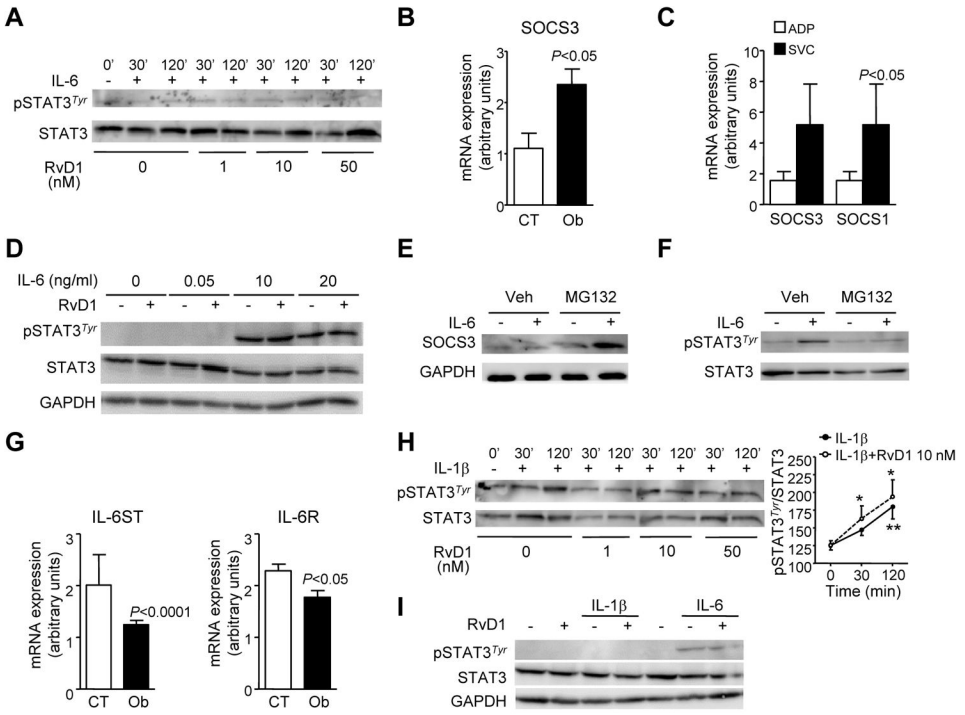

Figure 5. Obese adipose tissue explants are not responsive to IL-6-induced STAT3 phosphorylation

(A) Representative immunoblots of STAT3 and STAT3 Tyr705 phosphorylation (pSTAT3^{Tyr}) assessed by western blot in adipose tissue explants incubated with increasing concentrations of RvD1 (0, 1, 10 and 50 nM) for 30 min followed by the addition of IL-6 (10 ng/ml) for 30 or 120 min. **(B)** SOCS3 mRNA expression in adipose tissue from control (CT, n=8) and obese (Ob, n=24) individuals. **(C)** mRNA expression for SOCS3 and SOCS1 was analyzed in adipocytes (ADP) and stromal vascular cells (SVC) isolated from human obese adipose tissue. **(D)** Representative immunoblot of STAT3 and pSTAT3^{Tyr} in THP-1 monocytes incubated in the absence (−) or presence (+) of RvD1 (10 nM) for 30 min followed by the addition of increasing concentrations of IL-6 for 10 min. **(E)** Representative immunoblots of SOCS3 and GAPDH in THP-1 cells pre-incubated with vehicle (0.2% ethanol) or MG132 (10 μM) for 30 min before the addition of IL-6 (10 ng/ml) for 5 h. **(F)** Representative immunoblots of STAT3 and pSTAT3^{Tyr} in THP-1 cells pre-incubated with IL-10 (20 ng/ml) for 30 min before the addition of IL-6 (10 ng/ml) in the presence of vehicle (0.2% ethanol) or MG132 (10 mM) for 5 h. **(G)** Relative mRNA levels for both IL-6 signal transducer (ST), also known as gp130, and IL-6 receptor (R) genes in human adipose tissue from CT (n=6) and Ob (n=18) subjects were assessed by real-time PCR relative to a calibrator sample consisting of a total RNA derived from normal human adipose tissue pooled from 18 individuals. **(H)** Representative inmmunoblots of STAT3 activation (left panel) assessed by western blot in adipose tissue explants incubated with increasing concentrations of RvD1 (0, 1, 10 and 50 nM) for 30 min followed by the addition of IL-1β (25 pg/ml) for 30 or 120 min and kinetic analysis of STAT3^{Tyr} phosphorylation (right panel) in adipose tissue explants incubated in the absence (solid circles) or presence (empty circles) of RvD1 (10 mM) and stimulated with IL-1β. **(I)** Representative immunoblots of STAT3 and pSTAT3^{Tyr} in THP-1-

derived macrophages incubated in the absence (−) or presence (+) of RvD1 (10 nM) for 30 min followed by the addition of either IL-1β (25 pg/ml) or IL-6 (10 ng/ml) for 10 min. Results are expressed as mean ± SEM of n=3 independent experiments performed in duplicate. *P* values are given vs CT or ADP. *, $P<0.05$ and **, $P<0.005$ vs vehicle (0.01% ethanol) at time 0.

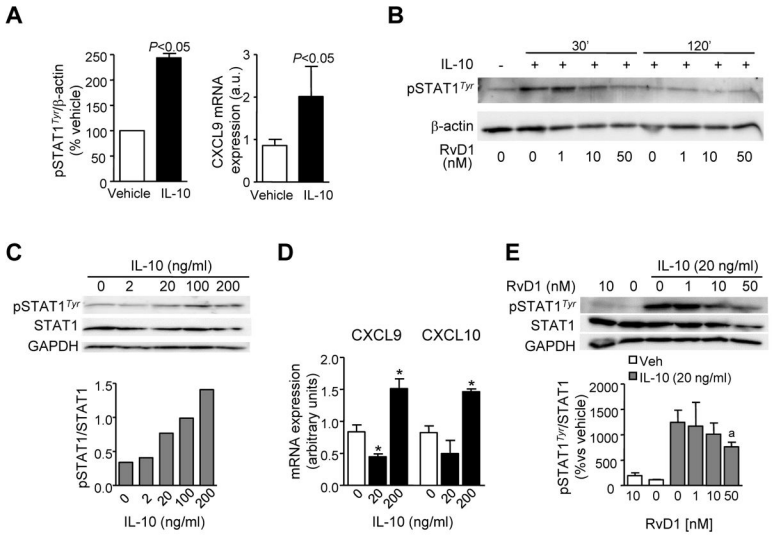

Figure 6. RvD1 attenuates IL-10-induced STAT1 activation in human obese adipose tissue and macrophages

(A) Levels of STAT1 Tyr701 phosphorylation (pSTAT1^{Tyr}) after 30 min of IL-10 stimulation and expression of its target gene CXCL9 in obese adipose tissue explants incubated for 6 h with IL-10 (20 ng/ml). **(B)** Representative inmunoblots of pSTAT1^{Tyr} and β-actin assessed by western blot in visceral adipose tissue explants incubated with increasing concentrations of RvD1 (0, 1, 10 and 50 nM) for 30 min followed by the addition of IL-10 (20 ng/ml) for 30 or 120 min**. (C)** Representative immunoblots analyzing STAT1 activation in THP1 monocytes incubated in the presence of increasing concentrations of IL-10 for 10 min. Densitometric analysis of phosphorylated protein to total protein ratios is shown below. **(D)** mRNA expression for STAT1 target genes (CXCL9 and CXCL10) in THP1-derived macrophages incubated in the presence of increasing concentrations of IL-10 for 6 h. **(E)** Representative immunoblots of STAT1 and pSTAT1^{Tyr} in THP-1-derived macrophages incubated in the presence of increasing concentrations of RvD1 for 30 min followed by the addition of IL-10 (20 ng/ml) for 10 min. Densitometric analysis of phosphorylated protein to total protein ratios is shown below. Results are expressed as mean ± SEM of n=3 independent experiments performed in duplicate. *P* values are given vs vehicle. *, $P<0.05$ vs vehicle, [a], $P<0.05$ vs IL-10-treated cells.

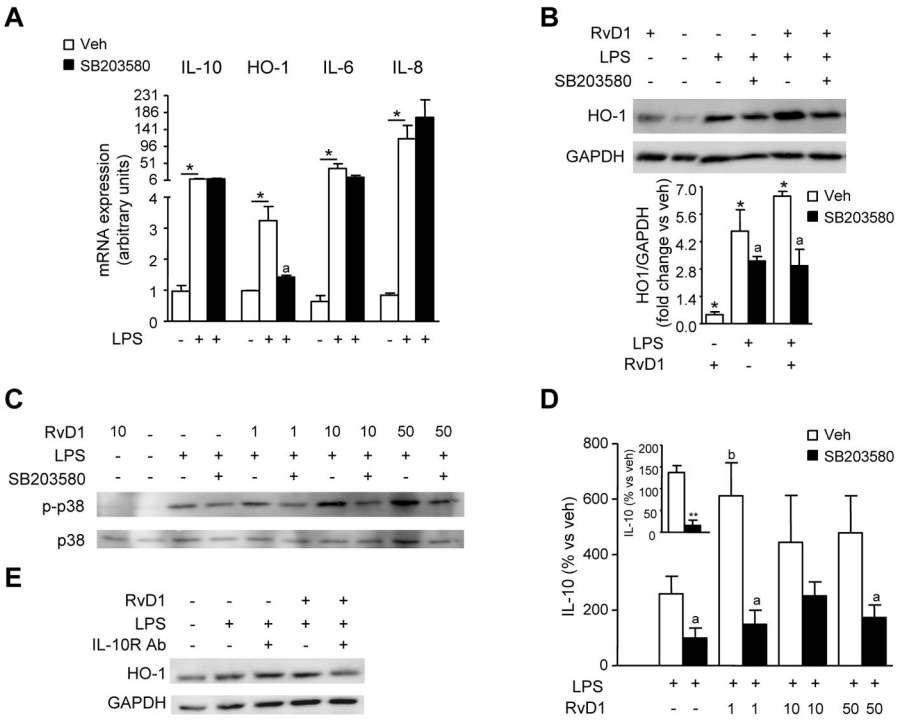

Figure 7. RvD1 enhances the production of HO-1 and IL-10 by a p38 MAPK-dependent mechanism in human monocytes

(A) mRNA expression for IL-10, HO-1, IL-6 and IL-8 in THP-1 cells pre-incubated with the p38 MAPK inhibitor SB203580 (5 μM) for 30 min before the addition of LPS (1 μg/ml) for 6 h. **(B)** Representative inmunoblot and densitometric analysis of HO-1 protein expression in THP-1 cells pre-incubated with RvD1 (10 nM) in the presence or absence of SB203580 (5 μM) for 30 min before the addition of LPS (1 μg/ml) for 6 h. **(C)** Representative immunoblots of p38 MAPK and its phosphorylated form (p-p38, phosphorylation at Thr180/Tyr182) in THP-1 cells pre-incubated with RvD1 (1, 10 and 50 nM) and SB203580 (5 μM) for 30 min before the addition of LPS (1 μg/ml) for 6 h. **(D)** IL-10 levels in supernatants of cultured human obese adipose tissue explants pre-incubated with the p38 MAPK inhibitor SB203580 (5 μM) in the presence of increasing concentrations of RvD1 for 30 min before the addition of LPS (1 μg/ml) for 24 h were detected by a specific ELISA kit (see Materials and Methods for details). Basal IL-10 levels in untreated (empty bar) and RvD1 (10 nM)-treated cells (solid bar) are shown in the insert. Protein levels are shown as the percentage of IL-10 production relative to untreated tissue explants. **(D)** Representative immunoblot of HO-1 in THP-1 cells incubated with RvD1 (10 nM) for 30 min before the addition of LPS (1 μg/ml) in the presence or absence of a neutralizing antibody to IL-10 receptor (10 μg/ml) for 6 h. Results are expressed as mean ± SEM. *, $P<0.05$ compared with LPS-untreated cells, **, $P<0.005$ compared with vehicle, [a], $P<0.05$ vs its paired LPS-stimulated cells without SB203580 pre-treatment, [b], $P<0.05$ vs LPS-treated cells.

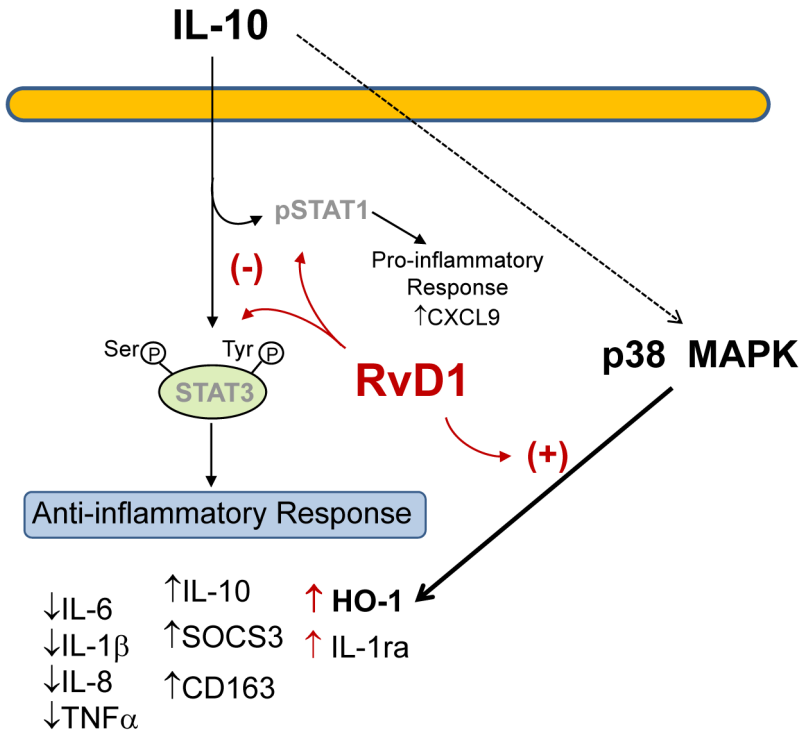

Figure 8. Schematic diagram of the interaction of RvD1 with the IL-10 signaling pathway

IL-10 promotes a STAT3-mediated anti-inflammatory response characterized by reduced expression of pro-inflammatory cytokines and increased expression of anti-inflammatory targets. Persistent activation of STAT signaling by IL-10 results in a pro-inflammatory response characterized by the up-regulation of STAT1-dependent CXCL9 target. In these conditions, RvD1 limits excessive overactivation of the STAT pathway while maintaining the IL-10-induced anti-inflammatory response via positive regulation of HO-1 through the p38 MAPK pathway. The p38 MAPK pathway also signals the actions of RvD1 on IL-1ra, a natural inhibitor of the pro-inflammatory actions of IL-1β.